Structural Dependence of Microwave Dielectric Properties of $SrRAlO_4$ (R = Sm, Nd, La) Ceramics: Crystal Structure Refinement and Infrared Reflectivity Study

Xie Cheng Fan, Xiang Ming Chen,* and Xiao Qiang Liu

Department of Materials Science & Engineering, Zhejiang University, Hangzhou 310027, China

Received November 16, 2007. Revised Manuscript Received March 27, 2008

The crystal structure refinement and infrared reflectivity study were carried out for $SrRAlO_4$ (R = Sm, Nd, La) ceramics with K_2NiF_4 structure to investigate the correlations between the crystal structure, polar-phonon mode parameters, and microwave dielectric properties. Fourier transform infrared reflectivity spectra in the range of 50−4000 cm^{-1} were measured and evaluated by means of classical oscillator fit. The data were extrapolated below the measured frequency range to estimate the intrinsic microwave losses. Heavy distortions of $(Sr,R)O_9$ dodecahedra and AlO_6 octahedra are observed in the crystal structure and they should attribute to interlayer electric polarization and interlayer size mismatch. The two lowest-frequency polar-phonon modes, which give primary contributions to the microwave complex permittivity, are the bending and stretching vibrations of (Sr,R)-AlO_6, so that the distortion of $(Sr,R)O_9$ dodecahedra has a great impact on the dispersion parameters of these two modes and consequently affects polarizabilities and intrinsic dielectric losses of $SrRAlO_4$ greatly. The above findings provide the general guideline for modifying the intrinsic microwave dielectric properties for $SrRAlO_4$ ceramics. Moreover, the calculated $Q \times f$ values are 25 000−85 000 GHz higher than the measured ones, and this suggests the great opportunity to improve $Q \times f$ through optimizing the microstructures.

Introduction

Since the 1970s, dielectric materials have been developed and put into practical use for resonators, filters and oscillators at microwave frequencies. The growth of the mobile phone market in the 1990s led to extensive research and development in this area. To meet the industrial requirements, current development trends of microwave dielectric ceramics are (1) reducing the cost by developing new materials without noble elements such as Ta and Nb, (2) reducing the extrinsic dielectric loss, and (3) lowering the sintering temperature for cofiring with metal electrodes.[1–3] Meanwhile, increasing efforts have been devoted to the study of intrinsic factors that affect the microwave dielectric properties,[3–9] especially for the complex perovskites with 1:2 ordering on B-site. For developing better materials, it is a key issue to reveal the universal relationships between the dielectric properties and crystal structure.

$ABCO_4$ layered compounds with K_2NiF_4 structure (see Figure 1) are important dielectric materials. $CaNdAlO_4$, $SrLaAlO_4$, $SrLaGaO_4$, and $SrPrGaO_4$ single crystals, which have excellent microwave dielectric properties, are used as substrates for high-temperature superconductive thin films.[10,11] Recently, $MRAlO_4$ (M = Ca, Sr; and R = Y, La, Nd, Sm) ceramics were proposed as the promising candidates of low-loss microwave dielectric ceramics.[12–14] The crystal structures were refined for $CaYAlO_4$, $CaNdAlO_4$, $SrLaAlO_4$,

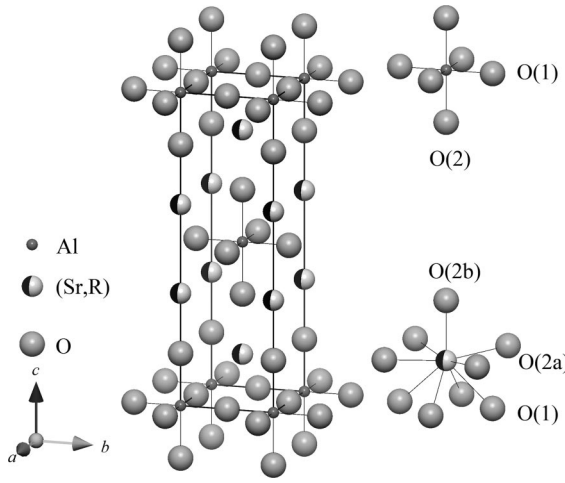

Figure 1. Polyhedral representations of the K_2NiF_4 structure of $SrRAlO_4$ (R = Sm, Nd, La) ceramics.

* Corresponding author. E-mail: xmchen59@zju.edu.cn. Tel/Fax: 86 (571) 87952112.

(1) Vanderah, T. A. *Science* **2002**, *298*, 1182.
(2) Cruichshank, D. *J. Eur. Ceram. Soc.* **2003**, *23*, 2721.
(3) Reaney, I. M.; Iddles, D. *J. Am. Ceram. Soc.* **2006**, *89*, 2063.
(4) Lufaso, M. W. *Chem. Mater.* **2004**, *16*, 2148.
(5) Zurmühlen, R.; Petzelt, J.; Kamba, S.; Voitsekhovskii, V. V.; Colla, E.; Setter, N. *J. Appl. Phys.* **1995**, *77*, 5341.
(6) Moreira, R. L.; Matinaga, F. M.; Dias, A. *Appl. Phys. Lett.* **2001**, *78*, 428.
(7) Surendran, K. P.; Sebastian, M. T.; Mohanan, P.; Moreira, R. L.; Dias, A. *Chem. Mater.* **2005**, *17*, 142.
(8) Wu, H.; Davies, P. K. *J. Am. Ceram. Soc.* **2006**, *89*, 2250.
(9) Jancar, B.; Valant, M.; Suvorov, D. *Chem. Mater.* **2004**, *16*, 1075.
(10) Pajaczkowska, A.; Gloubokov, A. *Prog. Cryst. Growth Charact.* **1998**, *36*, 123.
(11) Krupka, J.; Derzakowski, K.; Tobar, M.; Hartnett, J.; Geyer, R. *Meas. Sci. Technol.* **1999**, *10*, 387.
(12) Liu, X. Q.; Chen, X. M.; Xiao, Y. *Mater. Sci. Eng., B* **2003**, *103*, 276.
(13) Chen, X. M.; Xiao, Y.; Liu, X. Q.; Hu, X. *J. Electroceram.* **2003**, *10*, 111.
(14) Xiao, Y.; Chen, X. M.; Liu, X. Q. *J. Am. Ceram. Soc.* **2004**, *87*, 2143.

10.1021/cm703273z CCC: $40.75
Published on Web 05/17/2008

etc.,[15] and the synthesis, growth, and characterization of these tetragonal $ABCO_4$ crystals were summarized in a review.[10] However, many questions concerning the relation between the intrinsic dielectric properties and crystal structure remain unresolved.

At microwave frequencies, the overall dielectric loss is divided into the intrinsic loss part and the extrinsic loss part. The intrinsic part is the loss in a crystal without imperfection due to the anharmonic interaction of a.c. electric field with the phonon system of the crystal, whereas the extrinsic part originates from the defects and microstructure flaws, such as the porosity, secondary phase, grain boundaries, and impurities. It is an important issue to determine the intrinsic loss because one can know the improvement limit of Q value by controlling the extrinsic loss through optimizing the microstructures after determining the intrinsic dielectric loss (theoretic) and the total dielectric loss (measured). Also, it is important to reveal the relations between the intrinsic loss and structural parameters. On the other hand, the temperature coefficients of resonant frequency were often discussed in terms of octahedral tilting or dilution of the average ionic polarizability for perovskites.[16,17] However, in the compounds with K_2NiF_4 structure, octahedral tilting does not exist and the lattice strains result in the large polyhedral distortions, and therefore τ_f of these compounds should differ from those for the perovskites.

To understand the nature of the low-loss microwave dielectric materials in terms of phonon modes, the analysis of far and middle infrared reflectivity spectroscopy is widely used, where the infrared reflectivity spectra are analyzed with the classical oscillator model or the generalized four-parameter oscillator model.[5,18,19] The study on the relations among structural parameters, polar-phonon modes parameters, and dielectric properties has not been reported for $MRAlO_4$ compounds before.

In the present work, the structural dependence of intrinsic dielectric properties of $SrRAlO_4$ (R = Sm, Nd, La) ceramics at microwave frequencies is primarily investigated through the crystal structural refinement, bond valence analysis, and infrared reflectivity study.

Experimental Methods

Sample Synthesis. Single-phase $SrRAlO_4$ (R = Sm, Nd, La) ceramics were prepared by a solid-state reaction process, using high-purity $SrCO_3$ (99.9%), Sm_2O_3 (99.9%), Nd_2O_3 (99.9%), La_2O_3 (99.99%), and Al_2O_3 (99.99%) powders as the raw materials. The weighed raw materials were mixed, by ball milling with zirconia media, in ethanol for 24 h. The mixtures were calcined at 1250−1300 °C in air for 3 h after drying. The calcined powders were added with 7−8 wt % PVA (polyvinyl alcohol) water solution and were pressed into disks of 12 mm in diameter and 2−6 mm in height. The green disks were densified after sintered at 1500 °C in air for 3 h.

Table 1. D_0 Values and Effective Ionic Radii Used in This Work for the Bond between a Cation and Oxygen

	Sr^{2+}	Sm^{3+}	Nd^{3+}	La^{3+}	Al^{3+}	O^{2-}
coordination number N	9	9	9	9	6	6
D_0 (Å)	2.118	2.088	2.105	2.172	1.651	
effective ionic radius (Å)	1.31	1.132	1.163	1.216	0.535	1.40

Crystal Structure Refinement. Using an X-ray diffractometer (ARLX'TRA, Thermo Electron, Waltham, MA), the X-ray powder diffraction patterns were recorded in the 2θ range of 10−130° at a step width of 0.02° with dwelling time of 1s for each step. Structure refinements were carried out by the Rietveld method using the FULLPROF program.[20]

The bond-length, D_{ij}, and the bond-valence, S_{ij}, are correlated using the empirical equation of the bond-valence model[21,22]

$$S_{ij} = \exp\left(\frac{D_0 - D_{ij}}{B}\right) \quad (1)$$

where $B = 0.37$ and D_0 is the length of a bond of unit valence.[23,24] The discrepancy, d_i, between the sum of the bond valences around any atom, i, and its formal valence or oxidation state, V_i, can be expressed as

$$d_i = V_i - \sum_j S_{ij} \quad (2)$$

For most compounds, the value of d_i is usually small (<0.1 valence units (v.u.)), unless lattice effects cause excessive stretching or compression of the bonds. A measure of such lattice strains over the whole structure is the global instability index (GII),[25] which is the root-mean-square of the d_i values

$$\mathrm{GII} = \langle d_i^2 \rangle^{1/2} \quad (3)$$

Another measure of the stability of K_2NiF_4-type structure is the tolerance factor t defined for the perovskites as

$$t = \frac{(r_{Sr} + r_R)/2 + r_O}{\sqrt{2}(r_{Al} + r_O)} \quad \text{with } t > 0.87 \quad (4)$$

where r_{Sr}, r_R, r_{Al}, and r_O are the effective radii[26] of Sr, R, Al, and O ions, respectively. The tolerance factor in somewhat reflects the size adaptability between perovskite and rocksalt layers. The values of D_0, and effective ionic radii used in this work for the bond between a cation and oxygen are listed in Table 1.

Infrared Reflectivity Measurement and Classical Oscillator Analysis. Near-normal (angle of incidence 12°) reflectivity measurements were carried out at the room temperature using a Fourier-transform infrared spectrometer (IFS 66v/S Vacuum, Bruker Optik GmbH, Ettlingen, Germany) in the frequency ranges of 50−650 cm^{-1} (source: Hg lamp; beamsplitter: Multilayer Far IR/Mylar;

(15) Shannon, R. D.; Oswald, R. A.; Parise, J. B.; Chai, B. H. T.; Byszewski, P.; Pajaczkowska, A.; Sobolewski, P. *J. Solid State Chem.* **1992**, *98*, 90.
(16) Reaney, I. M.; Collar, E. L.; Setter, N. *Jpn. J. Appl. Phys.* **1994**, *33*, 3984.
(17) Wise, P. L.; Reaney, I. M.; Lee, W. E.; Iddles, D. M.; Cannell, D. S.; Price, T. J. *J. Mater. Res.* **2002**, *17*, 2033.
(18) Wakino, K.; Murata, M.; Tamura, H. *J. Am. Ceram. Soc.* **1986**, *69*, 34.
(19) Berreman, D. W.; Unterwald, F. C. *Phys. Rev.* **1968**, *174*, 791.
(20) Roisnel, T.; Rodriguez-Carvajal, J.; *Commission on Powder Diffraction Newsletter*; International Union of Crystallography: Chester, U.K., 2001; Vol. 26, p 12.
(21) Sanches-Salinas, A.; Garcia-Munoz, J. L.; Rodriguez-Carvajal, J.; Saez-Puche, R.; Martinez, J. L. *J. Solid State Chem.* **1992**, *100*, 201.
(22) Brown, I. D. *Acta Crystallgr. B* **1992**, *48*, 553.
(23) Brown, I. D.; Altermatt, D. *Acta Crystallogr., Sect. B* **1985**, *41*, 244.
(24) Brese, N. E.; O'Keeffe, M. *Acta Crystallogr., Sect. B* **1991**, *47*, 192.
(25) Rao, G. H.; Bärner, K.; Brown, I. D. *J. Phys.: Condens. Matter* **1998**, *10*, L757.
(26) Shannon, R. D. *Acta Crystallogr., Sect. A* **1976**, *32*, 751.
(27) Hakki, B. W.; Coleman, P. D. *IEEE Trans. Microwave Theory Tech.* **1960**, *8*, 402.

detector: DLATGS with polyethylene window) and 550−4000 cm^{-1} (source, SiC glowbar; beamsplitter, Ge multilayer coating on KBr; detector, DLATGS with KBr window) with a resolution of 2 cm^{-1}. The polished ceramic samples with flatness around 1μm were placed in a vacuum chamber at 2 mbar, and the reflectivity was obtained as the intensity relative to the reflectance of an evaporated gold mirror. The far and middle infrared spectra agreed well with one another in the overlapped frequency range. The absolute accuracy of the reflectivity measurement was about ±4%, which was estimated from the overlapping regions. The relative accuracy determined by the spectral noise was much better in most of the spectral range. Reflectivity spectra $R(\omega)$ are related to complex permittivity spectra $\varepsilon^*(\omega)$ by

$$R(\omega) = \left|\frac{\sqrt{\varepsilon^*(\omega)} - 1}{\sqrt{\varepsilon^*(\omega)} + 1}\right|^2 \quad (5)$$

According to the classical oscillator model,[5,18] the complex dielectric function $\varepsilon^*(\omega)$ can be written as

$$\begin{aligned}\varepsilon^*(\omega) &= \varepsilon_\infty + \sum_{j=1}^{n} \frac{S_j}{\omega_j^2 - \omega^2 + i\omega\gamma_j} \\ &= \varepsilon_\infty + \sum_{j=1}^{n} \frac{S_j(\omega_j^2 - \omega^2)}{(\omega_j^2 - \omega^2)^2 + \omega^2\gamma_j^2} - i\sum_{j=1}^{n} \frac{S_j\omega\gamma_j}{(\omega_j^2 - \omega^2)^2 + \omega^2\gamma_j^2} \\ &= \varepsilon'(\omega) - i\varepsilon''(\omega)\end{aligned} \quad (6)$$

where ε_∞ is the dielectric constant caused by the electronic polarization at the optical frequencies; n is the number of transverse polar-phonon modes; ω_j, S_j, and γ_j are the eigen frequency, strength, and damping constant of the jth mode, respectively; $\varepsilon'(\omega)$ and $\varepsilon''(\omega)$ are the real and image parts of the complex dielectric function, respectively. The obtained infrared reflectivity spectra were transformed into the complex dielectric spectra by means of the Kramers−Kroning analysis. The image part of the complex dielectric spectra was fitted with $\varepsilon''(\omega)$ in eq 6 to determine the initial values of ω_j, S_j, and γ_j for the following least-squares fit. The initial value of ε_∞ was estimated from the reflectivity at 4000 cm^{-1} using eq 5. Starting with these initial values, the infrared reflectivity spectra were fitted with eqs 5 and 6 to obtain the least-squares solution of dispersion parameters. The microwave dielectric constant and dielectric loss can be estimated under the condition of $\omega \ll \omega_j$:

$$\varepsilon'(\omega) = \varepsilon_\infty + \sum_{j=1}^{n} \Delta\varepsilon'_j = \varepsilon_\infty + \sum_{j=1}^{n} \frac{S_j}{\omega_j^2} \quad (7)$$

$$\tan\delta = \frac{\varepsilon''(\omega)}{\varepsilon'(\omega)} = \sum_{j=1}^{n} \Delta\tan\delta_j = \sum_{j=1}^{n} \frac{\omega}{\varepsilon'(\omega)} \frac{S_j\gamma_j}{\omega_j^4} \quad (8)$$

where $\Delta\varepsilon'_j$ and $\Delta\tan\delta_j$ denote the contributions of the jth mode to the dielectric constant and the dielectric loss at microwave frequencies, respectively.

Microwave Dielectric Property Measurement. The microwave dielectric constant ε_r and the temperature coefficient of resonance frequency τ_f were measured around 10 GHz by the Hakki-Coleman method[27] with a network analyzer (E8363B, Agilent Technologies Inc., Palo Alto, CA). The quality factor Q of the samples was evaluated around 7 GHz with the $TE_{01\delta}$ mode in a silver-coated cavity connected to the analyzer.[28] Because the Q-factor generally varies inversely with frequency (f) in the microwave region, the product $Q \times f$, rather than Q alone, was used to evaluate the dielectric loss.

Table 2. Refined Structural Parameters, Reliability Factors, Tolerance Factors, and Global Instability Index (GII) for $SrRAlO_4$ (R = Sm, Nd, La)[a]

	$SrSmAlO_4$	$SrNdAlO_4$	$SrLaAlO_4$
a(Å)	3.70869(5)	3.72412(5)	3.75699(4)
c(Å)	12.41782(17)	12.48558(20)	12.63626(12)
c/a	3.3483	3.3526	3.3634
(Sr,R) z	0.35827(6)	0.35868(5)	0.35879(4)
O(2) z	0.16551(45)	0.16407(38)	0.16323(27)
R_p	0.0852	0.0820	0.0819
R_{wp}	0.118	0.116	0.115
R_B	0.0914	0.0897	0.0844
χ^2	1.66	1.68	1.84
Al−O(1) (Å)	1.8543(0)	1.8621(0)	1.8785(0)
Al−O(2) (Å)	2.0551(62)	2.0489(50)	2.0622(38)
(Sr,R)−O(1) (Å)	2.5566(5)	2.5653(5)	2.5909(3)
(Sr,R)−O(2a) (Å)	2.6390(7)	2.6487(5)	2.6711(4)
(Sr,R)−O(2b) (Å)	2.3938(63)	2.4294(51)	2.4715(38)
$[(Sr,R)-O(2a)]_c$ (Å)[b]	0.2955	0.2847	0.2738
tolerance factor	0.958	0.964	0.973
GII	0.392	0.375	0.304

[a] The fixed atomic fractional coordinate positions are (Sr,R)[4e] (0, 0, z), Al[2a] (0, 0, 0), O(1)[4c] (0, 1/2, 0), and O(2)[4e] (0, 0, z) in space group $I4/mmm$. [b] The subscript c means the projected length along the c axis.

Results and Discussion

Crystal Structures, Coordination, and Bonding. The refined structural parameters, reliability factors, and tolerance factors for $SrRAlO_4$ (R = Sm, Nd, La) are listed in Table 2. The lattice parameters (a, c, and c/a), cation-oxygen interatomic distances, and tolerance factor increase with increasing the effective ionic radius of the rare earth cation (Sm^{3+} < Nd^{3+} < La^{3+}). For each compound of $SrRAlO_4$ (R = Sm, Nd, La), the AlO_6 octahedra are elongated along the c axis ($D_{Al-O(2)} \gg D_{Al-O(1)}$), whereas the $(Sr,R)O_9$ dodecahedra are compressed in this direction ($D_{(Sr,R)-O(2a)} \gg D_{(Sr,R)-O(1)} \gg D_{(Sr,R)-O(2b)}$).

The compression/dilation effects of different cation−oxygen bonds can be characterized by the normalized bond length, i.e., the ratio of the actual bond length to the ideal bond length given by the sum of the effective ionic radii. Figure 2 illustrates the compression/dilation effect of different cation-oxygen bonds as a function of the tolerance factor t. For each compound of $SrRAlO_4$ (R = Sm, Nd, La), the large differences between two kinds of Al−O bonds and among three kinds of (Sr,R)−O bonds are determined by the size adaption of the packing structure and the interlayer electric polarization.[29,30]The tolerance factor is smaller than 1 in $SrRAlO_4$ (R = Sm, Nd, La), so that in the ab plane, the (Sr,R)−O(2a) bonds tend to be lengthened while the Al−O(1) bonds tend to be shortened; accordingly, the Al−O(2) bonds along the c axis are elongated. On the other hand, the sequence of the formal charges of the alternating layers along the c axis, −AlO−(Sr,R)O−(Sr,R)O−AlO_2−(Sr,R)O−(Sr,R)O−, can be expressed as −(−1)−(+0.5)−(+0.5)−(−1)−(+0.5)−(+0.5)−, which reflects the interlayer polarizations. To minimize the

(28) Fan, X. C.; Chen, X. M.; Liu, X. Q. *IEEE Trans. Microwave Theory Tech.* **2005**, *53*, 3130.

(29) Magrez, A.; Cochet, M.; Joubert, O.; Louarn, G.; Ganne, M.; Chauvet, O. *Chem. Mater.* **2001**, *13*, 3893.

(30) Benabbas, A. *Acta Crystallogr., Sect. B* **2006**, *62*, 9.

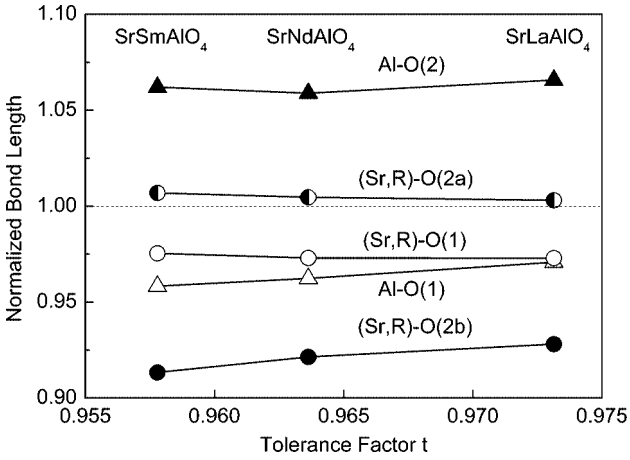

Figure 2. Compression and dilation effects of selected bonds versus corresponding tolerance factors.

interlayer polarizations, (Sr,R) cations move toward the neighboring $-AlO_2-$ layer with O(2) anions moving in the opposite direction, consequently the Al−O(2) and (Sr,R)−O(2a) bonds are elongated, whereas the Al−O(1), (Sr,R)−O(1), and (Sr,R)−O(2b) bonds are compressed. Because there are four (Sr,R)−O(1) bonds but only one (Sr,R)−O(2b) bond in a $(Sr,R)O_9$ dodecahedron, the (Sr,R)−O(2b) bonds are compressed much more heavily than the (Sr,R)−O(1) bonds. It is obvious that the sum of displacements of (Sr,R) and O(2) along the *c* axis, denoted as $[(Sr,R)-O(2a)]_c$ in Table 2, can reflect the reduction of the interlayer polarization in some measure.

When *t* approaches 1, stresses between the (Sr,R)−O(2a) bonds and the Al−O(1) bonds are to some extent released, as shown in Figure 2, but the variations are relatively small if compared with the large differences among the five different cation−oxygen bonds. So the interlayer polarization should take the major responsibility for the heavy distortion of the five different cation−oxygen bonds.

The calculated bond valence and bond valence sum (BVS) of any atom in $SrRAlO_4$ (R = Sm, Nd, La) are divided by their formal valence values to obtained normalized values, and the results are shown in Figure 3a and Figure 3b, respectively. Any bond or atom with a normalized valence value lager than 1 is compressed, otherwise is elongated or rattling. As shown in Figure 3a, R−O(2a), R−O(1), and Al−O(2) bonds are elongated, whereas other bonds, especially Sr−O(2b) bonds, are compressed. It is noteworthy in Figure 3b that heavily compressed Sr and very rattling R cations coexist at the A sites, and Al cations are a little rattling at the B sites. As the composition varies from $SrSmAlO_4$, $SrNdAlO_4$ to $SrLaAlO_4$, the overall distortion is reduced, as indicated by the global instability indices in Table 2.

Infrared Reflectivity Study. The site group analysis[31] of K_2NiF_4-type structure with *I4/mmm* space group gives the vibrational representations at the Γ point of the Brillouin zone: $\Gamma = 2A_g + 2E_g + 4A_{2u} + 5E_u + B_{2u}$, where $2A_g + 2E_g$ modes are Raman active, $3A_{2u} + 4E_u$ modes are infrared active, $A_{2u} + E_u$ modes are acoustic modes, and the B_{2u} mode is silent.

(31) Rousseau, D. L.; Bauman, R. P.; Porto, S. P. S. *J. Raman Spectrosc.* **1981**, *10*, 253.

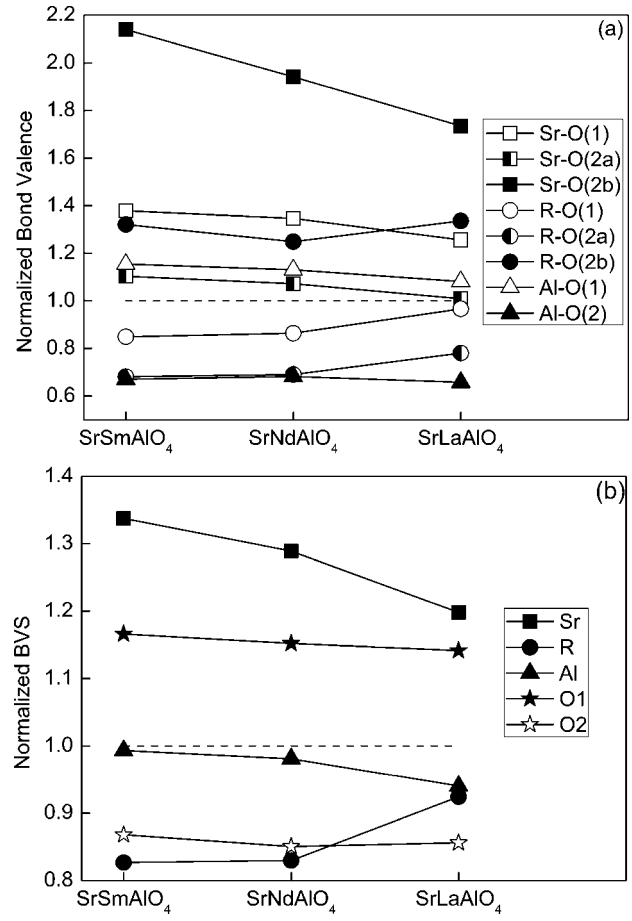

Figure 3. (a) Normalized bond valence of each cation and (b) normalized bond valence sum of each ion.

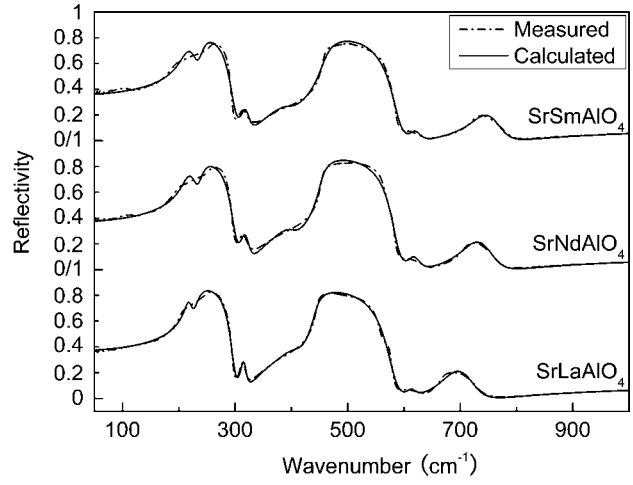

Figure 4. Measured and calculated infrared reflectivity spectra of $SrRAlO_4$ (R = Sm, Nd, La).

Figure 4 shows the infrared reflectivity spectra of the $SrRAlO_4$ (R = Sm, Nd, La) ceramics and these spectra were fitted with seven modes (j = 1, 2, ..., 7) in accordance with the site group analysis, and the calculated reflectivity spectra agree with the measured ones very well with standard deviations of 0.005−0.007. The dispersion parameters obtained by the principle of least-squares are listed in Table 3.

The two polar-phonon modes with the lowest frequencies (j = 1 and 2) give the primary contribution to the microwave

Table 3. Dispersion Parameters of the $SrRAlO_4$ (R = Sm, Nd, La) Series Obtained from Classical Oscillator Fit

compd	j	ω_j (cm^{-1})	γ_j (cm^{-1})	$\Delta\varepsilon'_j$	$\Delta\tan\delta_j \times 10^4$ @ 10 GHz
$SrSmAlO_4$	1	212	24.49	6.9	0.8102
	2	241	19.77	1.8	0.1352
	3	316	16.89	0.1	0.0048
	4	395	61.28	0.5	0.0436
	5	459	26.12	1.9	0.0517
	6	619	28.59	0.0	0.0004
	7	734	51.02	0.2	0.0045
	ε_∞			3.9	0.0000
	Σ			15.6	1.0504
$SrNdAlO_4$	1	213	21.02	7.4	0.6770
	2	239	18.67	2.3	0.1447
	3	315	17.42	0.2	0.0053
	4	396	52.34	0.7	0.0452
	5	453	16.77	2.0	0.0326
	6	614	27.10	0.0	0.0005
	7	717	51.61	0.2	0.0047
	ε_∞			4.1	0.0000
	Σ			16.9	0.9100
$SrLaAlO_4$	1	215	12.00	5.2	0.2688
	2	232	18.17	4.0	0.2683
	3	313	10.49	0.1	0.0024
	4	405	62.46	1.1	0.0852
	5	443	18.48	1.9	0.0352
	6	611	21.40	0.0	0.0002
	7	681	54.95	0.2	0.0054
	ε_∞			4.2	0.0000
	Σ			16.7	0.6656

Table 4. Measured and Calculated Dielectric Properties around 7−10 GHz

	measd				calcd	
composition	porosity (%)	ε_r[a]	$Q \times f$ (GHz)	τ_f (ppm/°C)	ε_r	$Q \times f$ (GHz)
$SrSmAlO_4$	5	18.3 (19.7)	70 000	−1	15.5	95 300
$SrNdAlO_4$	3	18.4 (18.9)	55 300	−15	16.9	110 000
$SrLaAlO_4$	2	17.6 (18.2)	65 500	−32	16.7	149 400

[a] The values before and in the parentheses are measured dielectric constants of real ceramics with pores and dielectric constants, which is calculated from the measured dielectric constant and porosity using the Maxwell−Wagner equation, of imaginary ceramics without pores, respectively.

dielectric constant (about 55%) and intrinsic dielectric loss (80−90%) at microwave frequencies. The dominant contribution of low-frequency modes to complex permittivity is based on the fact that for a given effective charge of a polar-phonon mode its contributions are $\Delta\varepsilon'_j \propto S_j\omega_j^{-2}$ and $\Delta\tan\delta_j \propto \omega S_j\gamma_j\omega_j^{-4}$, and decrease very fast with increasing ω_j.

Dielectric Constant and Polarizability. Table 4 shows microwave dielectric properties of $SrRAlO_4$ (R = Sm, Nd, La) ceramics measured around 7−10 GHz, together with the calculated dielectric constants and $Q \times f$ values. The calculated dielectric constants are in good agreement with the measured values.

The polarizability α_D can be evaluated based on the microscopic Clausius−Mosotti relationship

$$\alpha_D = \frac{3V_m}{4\pi}\frac{\varepsilon_r - 1}{\varepsilon_r + 2} \quad (9)$$

where, V_m is the molar volume in $Å^3$ (one-half of the unit-cell volume), ε_r is the dielectric constant of an ceramic sample without pores, which can be calculated from the measured dielectric constant and porosity of a real ceramic sample using the Maxwell−Wagner equation. Figure 5 compares the total molecular dielectric polarizabilities determined from the measured dielectric constant using eq 9 and from the oxide additivity law.[32] The measured polarizabilities are smaller than those predicted by the oxide additivity law, and as the tolerance factor approaches 1, the relative deviation increases from −3.7% for $SrSmAlO_4$ to −5.7% for $SrLaAlO_4$. Such a great deviation should attribute to the great distortion of the crystal structure, especially $(Sr,R)O_9$ dodecahedra. The lowest frequency mode is an E_u mode and the second one is an A_u mode, and they are corresponding to the ionic vibrations of $(Sr,R)-AlO_6$ in the *ab* plane and along the *c* axis, respectively.[33−35] As shown in Figure 2, (Sr,R)−O(2a) bonds are nearly undistorted, whereas (Sr,R)−O(2b) and (Sr,R)−O(1) are heavily compressed, so the overall contribution of these two modes to the dielectric constant is suppressed substantially. Because these two modes give a primary contribution to the dielectric constant, it is not surprising that the measured polarizability is evidently smaller than the predicted one. These reasons can also explain why in $CaYAlO_4$, $CaNdAlO_4$, and $SrLaAlO_4$ single crystals, the effects of A-site cations on polarizability deviation seem to be greater than that of Al.[15] As the tolerance factor decreases, (Sr,R)−O(2a) and (Sr,R)−O(1) bonds are slightly elongated, whereas (Sr,R)−O(2b) are slightly compressed; their overall effect reduces the deviation of the measured polarizability from the predicted one because in a $(Sr,R)O_9$ polyhedron, the numbers of the three different (Sr,R)−O bonds are respectively 4, 4, and 1.

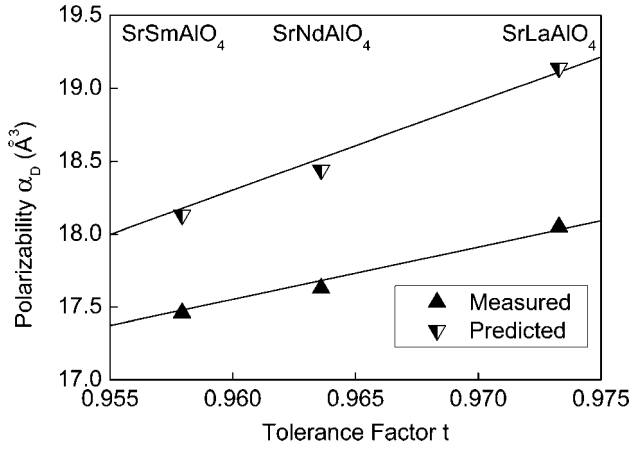

Figure 5. Measured and predicted values of polarizability versus the tolerance factor.

Dielectric Loss and $Q \times f$. As shown in Table 4, the calculated $Q \times f$ values are 25,000−85,000 GHz higher than the measured ones. This is because the dielectric losses measured at microwave frequencies include the extrinsic contributions aroused by the defects and microstructure flaw, such as charged defects, dislocations, grain boundaries, pores, etc., and most of these extrinsic contributions are excluded from the calculated ones (see the Supporting Information). Therefore, to minimize the extrinsic losses by improving processing techniques is important to improve $Q \times f$ values of $SrRAlO_4$ ceramics.

(32) Shannon, R. D. *J. Appl. Phys.* **1993**, *73*, 348.
(33) Hadjiev, V. G.; Cardona, M.; Ivanov, I.; Popov, V.; Gyulmezov, M.; Iliev, M. N.; Berkowski, M. *J. Alloys Compd.* **1997**, *251*, 7.
(34) Pintschovius, L.; Bassat, J. M.; Odier, P.; Gervais, F.; Chevrier, G.; Reichardt, W.; Gompf, F. *Phys. Rev. B* **1989**, *40*, 2229.
(35) Fennie, C. J.; Rabe, K. M. *Phys. Rev. B* **2003**, *68*, 184111.

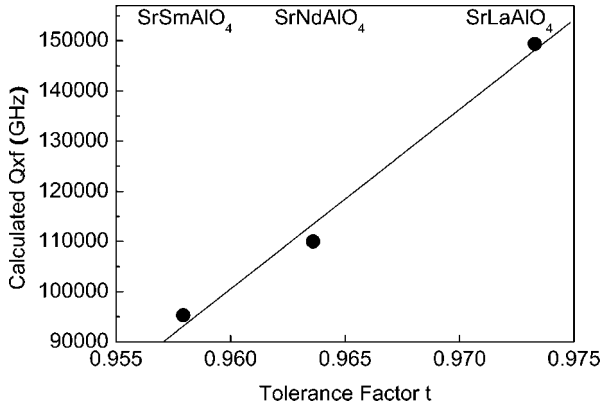

Figure 6. Calculated $Q \times f$ value of $SrRAlO_4$ (R = Sm, Nd, La) as a function of tolerance factor t.

The calculated $Q \times f$ value increases from 95 300 GHz to 149 400 GHz as the composition varies from $SrSmAlO_4$ to $SrLaAlO_4$, even though $SrSmAlO_4$ has a higher measured $Q \times f$ value than $SrLaAlO_4$. Figure 6 shows the relationship between the calculated $Q \times f$ value and the tolerance factor t: with t approaching 1, the calculated $Q \times f$ value increases linearly.

The variation of complex permittivity can be explained from the relations between polar-phonon mode parameters and structural characteristics. The dispersion parameters of the first mode are affected greatly by (Sr,R)−O(2a) and (Sr,R)−O(1) bonds, whereas those of the second mode mainly by (Sr,R)−O(2b). When t approaches 1, the normalized bond lengths of (Sr,R)−O(2a) and (Sr,R)−O(1) reduce, whereas that of (Sr,R)−O(2b) increases, just as shown in Figure 2, and these lead to an increase in ω_1 and $\Delta\varepsilon'_2$ but a decrease in $\Delta\varepsilon'_1$ and ω_2. For perovskite structures, if $t < 1$ (or $t > 1$), the size of the unit cell is determined by the B (or A) site ions so that the A (or B) site ions have too much room for vibrations and we expect lower eigenfrequencies and higher damping of modes involving A (or B) site ion vibrations. This empiristic conclusion held in many previous studies.[4,5,36] In the crystal structure of $SrRAlO_4$ (R = Sm, Nd, La), R−O(1), R−O(2a), and Al−O(2) bonds are elongated and under-bonded, as shown in Figure 3a, so that modes involving vibrations of these bonds are expected to become more damped. Therefore, the damping constant γ_1 of the first mode is very sensitive to the variation of the R−O(1) and R−O(2a) bonds: with t approaching 1, the normalized bond valences of the R-O(1) and R-O(2a) bonds approach 1, so γ_1 reduces greatly. As for the second mode, since Sr−O(2b) and R−O(2b) bonds are both compressed, γ_2 is not sensitive to their variation and just reduces slightly with increasing t.

Temperature Coefficient of Resonance Frequency (τ_f). On the basis of the macroscopic Clausius−Mosotti equation, an expression for the temperature coefficient of permittivity τ_ε at constant pressure is derived as[37]

$$\tau_\varepsilon = \frac{1}{\varepsilon_r}\left(\frac{\partial \varepsilon_r}{\partial T}\right) = \frac{(\varepsilon_r - 1)(\varepsilon_r + 2)}{3\varepsilon_r}\left[\frac{1}{\alpha_m}\left(\frac{\partial \alpha_m}{\partial T}\right)_V + \frac{1}{\alpha_m}\left(\frac{\partial \alpha_m}{\partial V}\right)_T\left(\frac{\partial V}{\partial T}\right)_P - \frac{1}{V}\left(\frac{\partial V}{\partial T}\right)_P\right] \quad (10)$$

where α_m is the polarizability of a macroscopic, small sphere with a volume V. The first term in the square brackets represents the direct dependence of the polarizability on temperature. In general, this is negative because of the anharmonic effect of the potential well in which an ion vibrates. The second term represents an increase of the polarizability of a constant number of dipoles with the increase of available volume as the temperature increases. The third term represents the direct effect of the volume expansion, i.e., a dilute of the concentration of dipoles as temperature increases. The sum of the last two terms, which describes the total effect of volume expansion, is found to be always positive.[37] τ_f is related to τ_ε and the linear thermal expansion coefficient α_L by

$$\tau_f = -\left(\frac{\tau_\varepsilon}{2} + \alpha_L\right) \quad (11)$$

In the Ruddlesden−Popper (RP) phases with general formula $Sr_{n+1}Ti_nO_{3n+1}$, the tuning of τ_f is attributed to the dilution of the average ionic polarizability, and an increase in ε_r of 1 leads to an increase in τ_f of 8 ppm/°C on average.[17] However, in $SrRAlO_4$ (R = Sm, Nd, La), an increase in ε_r of 1 leads to an increase in τ_f of around 20 ppm/°C. Moreover, a larger negative τ_f is observed in the present ceramics when the tolerance approaches 1, and this much differs from that in the perovskites.[16] This different dependence of τ_f upon the tolerance factor is worth investigating further.

Conclusion

In $SrRAlO_4$ (R = Sm, Nd, La) compounds with the K_2NiF_4 structure, AlO_6 octahedra and $(Sr,R)O_9$ dodecahedra are distorted greatly because of the interlayer electric polarization and interlayer size mismatch, and these are indicated by the large deviation of bond parameters from their ideal values, as well as large global instability indices, which exceed the usual upper limit for a stable crystal structure. This means that the K_2NiF_4-type crystal structure can accommodate unusually large crystal structure distortion and provides us with a great opportunity to study relationships between the crystal structures and dielectric properties. The two lowest-frequency polar-phonon modes, which give dominant contributions to microwave complex permittivity, are the bending and stretching vibrations of (Sr,R)-AlO_6, so that the distortion of $(Sr,R)O_9$ dodecahedra has a great impact on the dispersion parameters of the two polar-phonon modes and consequently affects the microwave dielectric properties greatly. The large distortion of $(Sr,R)O_9$ dodecahedra, is the major reason for the great deviation of measured polarizabilities from those predicted by the oxide additivity law. As the tolerance factor approaches 1, the distortion of $(Sr,R)O_9$ dodecahedra reduces and leads to a higher calculated $Q \times f$ values. To reduce the intrinsic microwave dielectric loss, it is important to adjust the tolerance factor close to 1 and to reduce the radius

(36) Petzelt, J.; Zurmühlen, R.; Bell, R.; Kamba, S.; Kozlov, G. V.; Volkov, A. A.; Setter, N. *Ferroelectrics* **1992**, *133*, 205.
(37) Bosman, A. J.; Havinga, E. E. *Phys. Rev.* **1963**, *129*, 1593.

difference between two kinds of cations on the A site. Moreover, the calculated $Q \times f$ values much higher than the measured ones suggest the great opportunity in the improvement of $Q \times f$ through optimizing the microstructures.

Acknowledgment. This work was partially supported by Chinese National Key Project for Fundamental Researches under Grant 2002CB613302, and National Science Foundation of China under Grant 50332030.

Supporting Information Available: Crystallographic information files (CIF), a table with Rietveld refinement parameters and isotropic thermal parameters for $SrSmAlO_4$, $SrNdAlO_4$, and $SrLaAlO_4$, and a discussion concerning the validity of calculated $Q \times f$ values using the classical oscillator model (PDF). This information is available free of charge via the Internet at http://pubs.acs.org.

CM703273Z